CW EC-QCL-based sensor for simultaneous detection of H_2O, HDO, N_2O and CH_4 using multi-pass absorption spectroscopy

Yajun Yu,[1, 3] Nancy P. Sanchez,[2] Robert J. Griffin,[2] and Frank K. Tittel[1]

[1]*Department of Electrical and Computer Engineering, Rice University, 6100 Main Street, Houston, TX 77005, USA*
[2]*Department of Civil and Environmental Engineering, Rice University, 6100 Main Street, Houston, TX 77005, USA*
[3]*School of Electronic Information, Wuhan University, Wuhan 430072, China*
[4]*yjy@rice.edu*
[5]*nps1@rice.edu*

Abstract: A sensor system based on a continuous wave, external-cavity quantum-cascade laser (CW EC-QCL) was demonstrated for simultaneous detection of atmospheric H_2O, HDO, N_2O and CH_4 using a compact, dense pattern multi-pass gas cell with an effective path-length of 57.6 m. The EC-QCL with a mode-hop-free spectral range of 1225-1285 cm^{-1} operating at ~7.8 μm was scanned covering four neighboring absorption lines, for H_2O at 1281.161 cm^{-1}, HDO at 1281.455 cm^{-1}, N_2O at 1281.53 cm^{-1} and CH_4 at 1281.61 cm^{-1}. A first-harmonic-normalized wavelength modulation spectroscopy with second-harmonic detection (WMS-2f/1f) strategy was employed for data processing. An Allan-Werle deviation analysis indicated that minimum detection limits of 1.77 ppmv for H_2O, 3.92 ppbv for HDO, 1.43 ppbv for N_2O, and 2.2 ppbv for CH_4 were achieved with integration times of 50-s, 50-s, 100-s and 129-s, respectively. Experimental measurements of ambient air are also reported.

OCIS codes: (280.3420) Laser sensors; (010.1280) Atmospheric composition; (300.6340) Spectroscopy, infrared; (140.5965) Semiconductor lasers, quantum cascade.

References and links

1. R. K. Pachauri, M. Allen, V. Barros, J. Broome, W. Cramer, R. Christ, J. Church, L. Clarke, Q. Dahe, and P. Dasgupta, "Climate Change 2014: Synthesis Report. Contribution of Working Groups I, II and III to the Fifth Assessment Report of the Intergovernmental Panel on Climate Change" (2014).
2. Y. Cao, N. P. Sanchez, W. Jiang, R. J. Griffin, F. Xie, L. C. Hughes, C. E. Zah, and F. K. Tittel, "Simultaneous atmospheric nitrous oxide, methane and water vapor detection with a single continuous wave quantum cascade laser," Opt. Express **23**(3), 2121–2132 (2015).
3. D. Noone, "Pairing measurements of the water vapor isotope ratio with humidity to deduce atmospheric moistening and dehydration in the tropical midtroposphere," J. Clim. **25**(13), 4476–4494 (2012).
4. S. A. Montzka, E. J. Dlugokencky, and J. H. Butler, "Non-CO_2 greenhouse gases and climate change," Nature **476**(7358), 43–50 (2011).
5. A. A. Kosterev, R. F. Curl, F. K. Tittel, C. Gmachl, F. Capasso, D. L. Sivco, J. N. Baillargeon, A. L. Hutchinson, and A. Y. Cho, "Effective utilization of quantum-cascade distributed-feedback lasers in absorption spectroscopy," Appl. Opt. **39**(24), 4425–4430 (2000).
6. D. D. Nelson, B. McManus, S. Urbanski, S. Herndon, and M. S. Zahniser, "High precision measurements of atmospheric nitrous oxide and methane using thermoelectrically cooled mid-infrared quantum cascade lasers and detectors," Spectrochim. Acta A Mol. Biomol. Spectrosc. **60**(14), 3325–3335 (2004).
7. M. Jahjah, W. Ren, P. Stefański, R. Lewicki, J. Zhang, W. Jiang, J. Tarka, and F. K. Tittel, "A compact QCL based methane and nitrous oxide sensor for environmental and medical applications," Analyst (Lond.) **139**(9), 2065–2069 (2014).
8. G. Hancock, J. Van Helden, R. Peverall, G. Ritchie, and R. Walker, "Direct and wavelength modulation spectroscopy using a cw external cavity quantum cascade laser," Appl. Phys. Lett. **94**(20), 201110 (2009).
9. J. Li, U. Parchatka, and H. Fischer, "A formaldehyde trace gas sensor based on a thermoelectrically cooled CW-DFB quantum cascade laser," Anal. Methods **6**(15), 5483–5488 (2014).
10. W. Ren, W. Jiang, and F. K. Tittel, "Single-QCL-based absorption sensor for simultaneous trace-gas detection of CH_4 and N_2O," Appl. Phys. B **117**(1), 245–251 (2014).

#262458 Received 4 Apr 2016; accepted 29 Apr 2016; published 3 May 2016

11. Y. Cao, N. P. Sanchez, W. Jiang, W. Ren, R. Lewicki, D. Jiang, and R. J. Griffin, "Multi-pass absorption spectroscopy for H_2O_2 detection using a CW DFB-QCL," Adv. Opt. Technol. **3**, 549–558 (2014).
12. G. Wysocki, R. F. Curl, F. K. Tittel, R. Maulini, J.-M. Bulliard, and J. Faist, "Widely tunable mode-hop free external cavity quantum cascade laser for high resolution spectroscopic applications," Appl. Phys. B **81**(6), 769–777 (2005).
13. G. Wysocki, R. Lewicki, R. Curl, F. Tittel, L. Diehl, F. Capasso, M. Troccoli, G. Hofler, D. Bour, S. Corzine, R. Maulini, M. Giovannini, and J. Faist, "Widely tunable mode-hop free external cavity quantum cascade lasers for high resolution spectroscopy and chemical sensing," Appl. Phys. B **92**(3), 305–311 (2008).
14. X. Chao, J. Jeffries, and R. Hanson, "Wavelength-modulation-spectroscopy for real-time, in situ NO detection in combustion gases with a 5.2 μm quantum-cascade laser," Appl. Phys. B **106**(4), 987–997 (2012).
15. K. Krzempek, M. Jahjah, R. Lewicki, P. Stefański, S. So, D. Thomazy, and F. K. Tittel, "CW DFB RT diode laser-based sensor for trace-gas detection of ethane using a novel compact multipass gas absorption cell," Appl. Phys. B **112**(4), 461–465 (2013).
16. L. Dong, Y. Yu, C. Li, S. So, and F. K. Tittel, "Ppb-level formaldehyde detection using a CW room-temperature interband cascade laser and a miniature dense pattern multipass gas cell," Opt. Express **23**(15), 19821–19830 (2015).
17. H. Li, A. Farooq, J. Jeffries, and R. Hanson, "Near-infrared diode laser absorption sensor for rapid measurements of temperature and water vapor in a shock tube," Appl. Phys. B **89**(2-3), 407–416 (2007).
18. L. Rothman, I. Gordon, Y. Babikov, A. Barbe, D. C. Benner, P. Bernath, M. Birk, L. Bizzocchi, V. Boudon, and L. Brown, "The HITRAN2012 molecular spectroscopic database," J. Quant. Spectrosc. Radiat. Transf. **130**, 4–50 (2013).
19. X. Liu, X. Zhou, A. Feitisch, and G. Sanger, "Pressure-invariant trace gas detection," U.S. Patent No. 7,508,521 (2009).
20. H. Li, G. B. Rieker, X. Liu, J. B. Jeffries, and R. K. Hanson, "Extension of wavelength-modulation spectroscopy to large modulation depth for diode laser absorption measurements in high-pressure gases," Appl. Opt. **45**(5), 1052–1061 (2006).
21. G. B. Rieker, J. B. Jeffries, and R. K. Hanson, "Calibration-free wavelength-modulation spectroscopy for measurements of gas temperature and concentration in harsh environments," Appl. Opt. **48**(29), 5546–5560 (2009).
22. D. Rehle, D. Leleux, M. Erdelyi, F. Tittel, M. Fraser, and S. Friedfeld, "Ambient formaldehyde detection with a laser spectrometer based on difference-frequency generation in PPLN," Appl. Phys. B **72**(8), 947–952 (2001).
23. M. Schneider, F. Hase, and T. Blumenstock, "Ground-based remote sensing of HDO/H_2O ratio profiles: introduction and validation of an innovative retrieval approach," Atmos. Chem. Phys. **6**(12), 4705–4722 (2006).
24. S. Kirschke, P. Bousquet, P. Ciais, M. Saunois, J. G. Canadell, E. J. Dlugokencky, P. Bergamaschi, D. Bergmann, D. R. Blake, L. Bruhwiler, P. Cameron-Smith, S. Castaldi, F. Chevallier, L. Feng, A. Fraser, M. Heimann, E. L. Hodson, S. Houweling, B. Josse, P. J. Fraser, P. B. Krummel, J.-F. Lamarque, R. L. Langenfelds, C. Le Quéré, V. Naik, S. O'Doherty, P. I. Palmer, I. Pison, D. Plummer, B. Poulter, R. G. Prinn, M. Rigby, B. Ringeval, M. Santini, M. Schmidt, D. T. Shindell, I. J. Simpson, R. Spahni, L. P. Steele, S. A. Strode, K. Sudo, S. Szopa, G. R. van der Werf, A. Voulgarakis, M. van Weele, R. F. Weiss, J. E. Williams, and G. Zeng, "Three decades of global methane sources and sinks," Nat. Geosci. **6**(10), 813–823 (2013).
25. I. Bamberger, J. Stieger, N. Buchmann, and W. Eugster, "Spatial variability of methane: attributing atmospheric concentrations to emissions," Environ. Pollut. **190**, 65–74 (2014).
26. L. Dong, C. Li, N. P. Sanchez, A. K. Gluszek, R. J. Griffin, and F. K. Tittel, "Compact CH_4 sensor system based on a continuous-wave, low power consumption, room temperature interband cascade laser," Appl. Phys. Lett. **108**(1), 011106 (2016).

1. Introduction

In recent decades atmospheric greenhouse gases (GHGs), such as water vapor, nitrous oxide (N_2O), and methane (CH_4), have contributed to climate forcing, which influences human and natural systems [1]. Water vapor is a primary energy carrier in the atmosphere and the dominant absorber and emitter of radiation regulating planetary temperatures [2]. An accurate knowledge of H_2O-HDO is relevant to identify different atmospheric processes that govern the moisture budget at specific locations [3]. Atmospheric N_2O has a steady-state lifetime of 120 yr and its mixing ratios, increasing at a rate of ~0.7 ppb/yr, are 19% higher than pre-industrial levels [4]. Methane is the most abundant non-carbon dioxide (CO_2) GHG and has a shorter steady-state lifetime in the atmosphere (~9 yr) than most other GHGs. Reduction in emissions of shorter-lived CH_4 decreases radiative forcing more rapidly [4]. Precise and sensitive detection of these relevant GHGs is critical to help assess mitigation efforts for global climate forcing.

Several optical sensing techniques using tunable diode laser absorption spectroscopy (TDLAS) have been employed for water vapor, N_2O and CH_4 detection. Kosterev et al.

#262458 Received 4 Apr 2016; accepted 29 Apr 2016; published 3 May 2016

reported a distributed-feedback (DFB) quantum cascade laser (QCL)-based gas sensor to detect CH_4, N_2O and some isotopic species of water in ambient air at 7.9 μm [5]. By using a 100m path-length multi-pass gas cell (MPGC), detection sensitivities of 2.5 ppb for CH_4, 1.0 ppb for N_2O and 60 ppb for H_2O were achieved with ~60-s data acquisition time. High precision measurements of N_2O and CH_4 were performed by a compact, fast response absorption spectrometer based on a thermoelectrically cooled (TEC) pulsed QCL and a MPGC with an optical path-length of 56m [6]. Simultaneous detection of N_2O and CH_4 at ~7.8 μm was achieved with root mean square noise levels of 3 ppb and 7 ppb, respectively with a 1-s averaging time. A compact quartz-enhanced photoacoustic absorption spectroscopy (QEPAS)-based senor platform was developed for environmental CH_4 and N_2O monitoring [7]. Detection limits for CH_4 at1275.04 cm^{-1} and N_2O at 1275.49 cm^{-1} were 13 ppb and 6 ppb, respectively, with a 1-s data acquisition time. Simultaneous measurements of atmospheric N_2O, CH_4 and water vapor were implemented by a 7.73-μm continuous wave CW DFB-QCL-based absorption sensor system employing a 76-m astigmatic MPGC with minimum detection limits (MDLs) of 1.7 ppb, 8.5 ppb, and 11 ppm for N_2O, CH_4, and H_2O, respectively, with a 2-s integration time for individual gas detection [2].

In this manuscript, we report the recent development of a laser absorption sensor for simultaneous monitoring of H_2O, HDO, N_2O, and CH_4 using a single CW external-cavity (EC) QCL operating at ~7.8 μm. An effective optical path-length of 57.6 m was achieved by using a compact MPGC (17 × 6.5 × 5.5 cm^3). Peak-to-peak amplitudes of second-harmonic signals demodulated from a lock-in amplifier were chosen and normalized by first-harmonic signals (WMS-$2f_{p\text{-}p}$/1f). The performance of the reported sensor system was evaluated for simultaneous multi-gas detection in atmospheric air.

2. EC-QCL characterization and sensor design

Development of CW QCLs has led to significant progress in mid-infrared spectroscopic detection of trace gases, due to their high output power, room temperature operation and inherently narrow linewidth [8]. Recently CW distributed feedback QCLs have been introduced in various gas-sensing applications [2, 5, 7, 9–11], but the spectral tuning range of the wavelength is limited to several wavenumbers by varying the temperature of the QCL chip and/or the QCL injection current. This thermal tuning impacts the QCL threshold and causes a decrease of the output power at higher QCL temperatures [12, 13]. The EC-QCL configuration, consisting of a QCL chip, a beam collimating lens, and a diffraction grating, can be used for selection of a QCL wavelength anywhere in a broad spectral gain region without changing the QCL chip temperature. A piezo-activated cavity-mode-tracking system is employed to provide independent control of the EC length and diffraction grating angle for wavelength scanning at low frequency. Rapid wavelength modulation can be performed by directly modulating the injection current of the QCL chip.

In our study, a water-cooled CW EC-QCL (Daylight Solutions, Model 21080-MHF) with a spectral tuning range from 1181 to 1290 cm-1 (mode-hop-free range of 1225-1285 cm-1) was used. Frequency calibration is required because an external sinusoidal waveform is used in piezo-electric (PZT) wavelength scanning [14]. Figure 1(a) depicts an example of the EC-QCL intensity variations through a germanium etalon (Team Photon, free spectral range of 0.0164 cm-1) with the center wavenumber at ~1275.8 cm-1. A laser controller (Daylight Solutions, Model 1001-TLC) was employed to set the QCL at a current of 400 mA. A function generator (Tektronix, AFG 3102) provided a sinusoidal waveform at a frequency of 1 Hz and a voltage amplitude of 2 V, which was applied to an external PZT driver (Thorlabs, MDT691) to adjust the EC system for laser frequency scanning. The peak positions from etalon interference fringes were extracted and fitted by a sinusoidal function to characterize the relative wavenumber variation shown in Fig. 1(b). This fitting yielded a coefficient of determination (R2) of 0.9995, indicating an excellent sinusoidal relationship between the relative wavenumber and the scanning time.

#262458 Received 4 Apr 2016; accepted 29 Apr 2016; published 3 May 2016

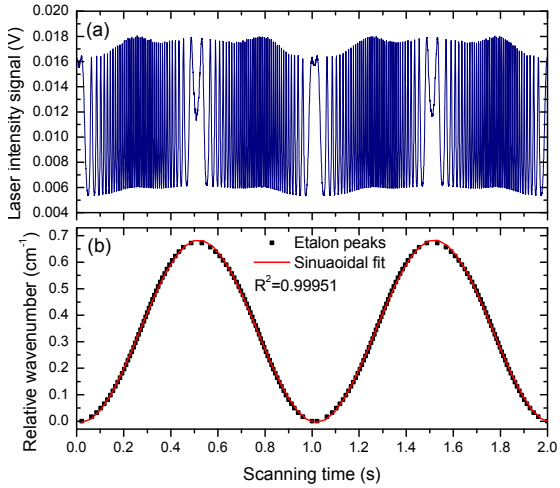

Fig. 1. EC-QCL intensity and wavenumber variation with a PZT scan at ~1275.8 cm^{-1} at 1 Hz scan rate.

The architecture of the four-gas species sensor system is depicted in Fig. 2. The CW EC-QCL emitting at ~7.8 μm was scanned by a combination of the function generator (scanning voltage amplitude 2 V and frequency 1 Hz) and the PZT driver described. A high-frequency (19 kHz) sinusoidal waveform generated by a lock-in amplifier (Stanford Research Systems, SR 830) was added to the QCL injection current (400 mA) to realize the EC-QCL wavelength modulation. The EC-QCL output radiation was directed to a wedged beam splitter and separated into three beams. The high-power (~150 mW) main beam was blocked by a beam dump. One of the reflected beams was co-aligned with a visible diode beam alignment laser (Coherent, λ = 630 nm) via a flip mirror. The combined laser beams were coupled into a 57.6-m MPGC (Sentinel Photonics) by means of a mode matching lens with a focal length of 200 mm. A dense spot pattern with minimized overlap can be created on the two mirror surfaces of the MPGC after 495 beam passes. The beam exiting the MPGC was focused onto a TE-cooled mercury-cadmium-telluride (MCT) detector (Vigo System S.A., PVIM-3TE-8) using a 40-mm focal length plano-convex lens. More details of the MPGC architecture can be found in [15, 16]. The electrical signal of the MCT detector was demodulated by two lock-in amplifiers to extract the 2f and 1f components, respectively, in order to implement a WMS-2f/1f strategy immune to laser intensity fluctuations [14, 17]. The processed data were subsequently acquired using a DAQ card (National Instruments, 6062E) and displayed by a Labview (National Instruments) interface in a laptop. The second reflected beam from the wedged beam splitter was passed through a 5-cm long reference cell (Thorlabs) filled with 1% N_2O and 0.5% CH_4 at 150 Torr and detected by a second mid-infrared detector (Vigo System S.A., PVM-10.6) to lock the laser wavelength at the N_2O absorption line located at 1281.53 cm^{-1}. A PID function-based Labview program controlling the offset voltage applied to the piezo element was implemented for wavelength locking. In the gas sampling system, a polytetrafluoroethylene filter (Pall Corporation, pore size 2.0 μm) was placed upstream to protect the spherical mirrors in the MPGC from potential contamination by dust, and a flow meter was connected to the inlet of the MPGC. The system pressure was maintained by a pressure controller (MKS Instruments, Type 640) and an oil free vacuum pump (Varian, DS 102) downstream to the MPGC.

#262458 Received 4 Apr 2016; accepted 29 Apr 2016; published 3 May 2016

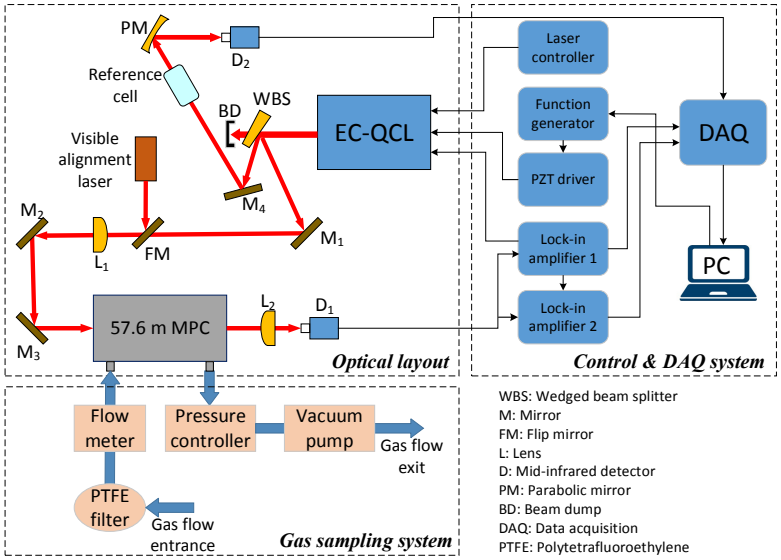

Fig. 2. Schematic of a CW EC-QCL based sensor system for simultaneous four trace gas species detection.

3. Selection of absorption lines

N_2O and CH_4 in the ν_1 and ν_4 fundamental vibrational bands, respectively, have strong spectral overlap between 7.5 and 8 μm [2, 10], as do H_2O and HDO at their ν_2 fundamental vibrational modes. Hence, these spectral features make it feasible to perform simultaneous four-gas monitoring using a single excitation laser source to reduce the size and cost of the reported mid-infrared sensor system. A spectral simulation of ambient air, with 1.5% water vapor (H_2O and HDO in a relative abundance of 0.9973 and 3.1×10^{-4}, respectively), 320 ppbv N_2O, 2 ppmv CH_4, 400 ppmv CO_2, and 10 ppbv NH_3 was plotted based on the HITRAN database [18] in the spectral range of 1281.05-1281.66 cm^{-1} as shown in Fig. 3(a) .Well resolved spectral features can be obtained at a gas pressure of 40 Torr, a temperature of 296 K and a path-length of 57.6-m. Four selected neighboring lines include a H_2O line (corresponding to two overlapped transitions) at 1281.161 cm^{-1}, a HDO line at 1281.454 cm^{-1}, a N_2O line at 1281.53 cm^{-1} and a CH_4 line at 1281.61 cm^{-1} and are well separated within a relatively narrow spectral region.

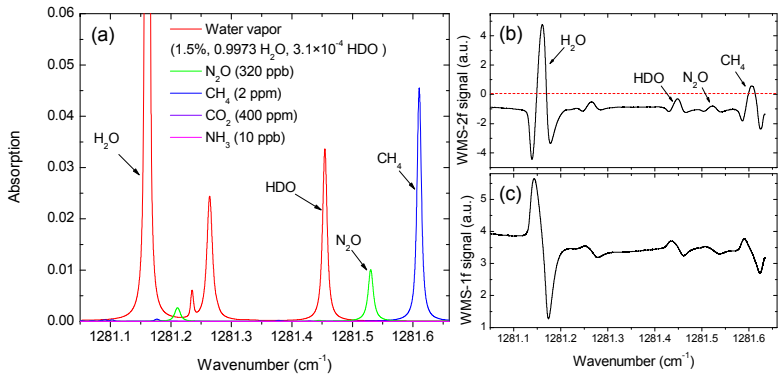

Fig. 3. (a) HITRAN simulation of absorption spectra of ambient air at 40 Torr, 296 K and 57.6 m path-length in the spectral range of 1281.05-1281.66 cm^{-1}; (b) 2f and (c) 1f signals from experimental measurements.

#262458 Received 4 Apr 2016; accepted 29 Apr 2016; published 3 May 2016

Experimental WMS-2f and 1f signals of ambient air were recorded and are depicted in Fig. 3(b) and 3(c). Due to the large nonlinearity in the EC-QCL intensity [14], the background 2f signal is non-zero in comparison with the dashed line of value zero illustrated in Fig. 3(b). The data processing algorithm selects the peak-to-peak amplitudes of absorption-induced 2f signals [19] and these are normalized by 1f signals selected at the same positions of the peak 2f signals [14, 17, 20, 21].

4. Sensor performance

4.1 Modulation optimization for simultaneous detection

The sensor system operation for simultaneous detection of H_2O, HDO, N_2O, and CH_4 at 40 Torr in the spectral range of 1281.05-1281.66 cm^{-1} is described in Sect. 2. The 2f and 1f signals were demodulated by two lock-in amplifiers with an optimum time constant of 30 ms. In order to optimize the detection sensitivity of the sensor system, the normalized WMS-$2f_{p-p}$/1f signals of the four gas species were measured at different modulation depths, varying from 0 to 2 V, plotted in Fig. 4. These measurements were conducted by using fixed gas-phase concentrations of water vapor (generated by a humidifier (PermSelect, PDMSXA-2500)), N_2O (1 ppm) and CH_4 (2 ppm). According to these test results, an optimum modulation depth occurs at 2 V. Further increases of this voltage are limited by the EC-QCL current-modulation design.

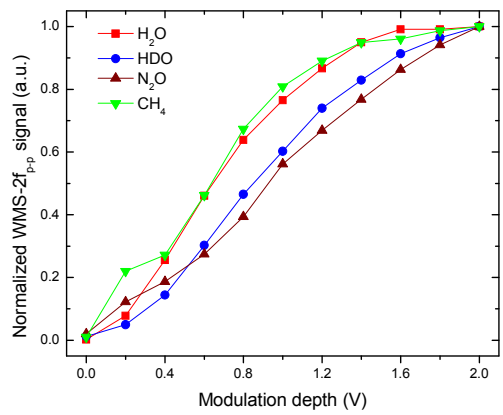

Fig. 4. Normalized WMS-$2f_{p-p}$/1f signals as a function of modulation depths for H_2O, HDO, N_2O, and CH_4 at 40 Torr.

4.2 Sensitivity calibration

The sensitivity calibration of the sensor system was performed by mixing pure nitrogen (N_2) with fixed concentrations of water vapor, N_2O, and CH_4 in the MPGC. Different water vapor mixing ratios were generated by controlling the air flow through a humidifier at eleven different flow rates, from 10 to 110 SCCM, and mixing with pure N_2 to reach a stable flow rate of 110 SCCM. The concentrations of both water isotopes at different flow rates were calculated by least-squares fitting of direct absorption curves to simulated Voigt profiles [22]. Figure 5(a) and 5(b) show water isotopic WMS-$2f_{p-p}$/1f signal responses of different concentrations. A quadratic polynomial fit is applicable to the H_2O sensitivity calibration (rather than a linear fit) because of its strong absorbance (0.05). The measured HDO signals have an excellent linear relationship (R^2 = 0.9996) with its concentrations. The N_2O and CH_4 sensitivity calibrations were carried out by diluting gases from two certified gas cylinders (2.1 ppmv N_2O:N_2 and 2 ppmv CH_4:N_2, respectively) with pure N_2 to generate different concentrations using a commercial gas dilution system (Environics, Series 4040). The N_2O and CH_4 WMS-$2f_{p-p}$/1f signals were plotted as a function of different concentration

#262458 Received 4 Apr 2016; accepted 29 Apr 2016; published 3 May 2016

levels and fitted by two lines as shown in Fig. 5(c) and 5(d), respectively. The coefficients of determination of these fittings are > 0.999, which indicates high stability and consistency of the EC-QCL based senor system for simultaneous four gas-species detection.

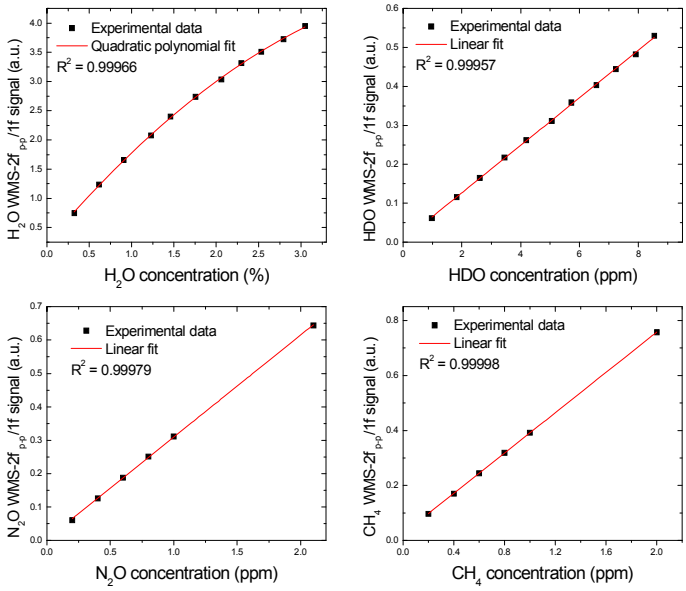

Fig. 5. Experimental WMS-$2f_{p\text{-}p}$/1f signals of (a) H_2O, (b) HDO, (c) N_2O, and (d) CH_4 as function of respective gas concentrations.

4.3 Noise level analysis

The noise level analysis of the reported TDLAS sensor system was determined by flowing pure N_2 through the MPGC and recording the WMS-$2f_{p\text{-}p}$/1f signals in terms of the four gas-species concentrations in a 2.3-hour period with 1-s time intervals. An Allan-Werle variance method was utilized to evaluate the long-term stability and precision of the sensor system, as depicted in Fig. 6. MDLs of 12.5 ppmv for H_2O, 26.5 ppbv for HDO, 17.0 ppbv for N_2O, and 24.0 ppbv for CH_4 were achieved with a 1-s integration time. Optimum MDLs were estimated to be 1.77 ppmv for H_2O, 3.92 ppbv for HDO, 1.43 ppbv for N_2O, and 2.2 ppbv for CH_4 with integration times at 50-s, 50-s, 100-s and 129-s, respectively.

#262458 Received 4 Apr 2016; accepted 29 Apr 2016; published 3 May 2016

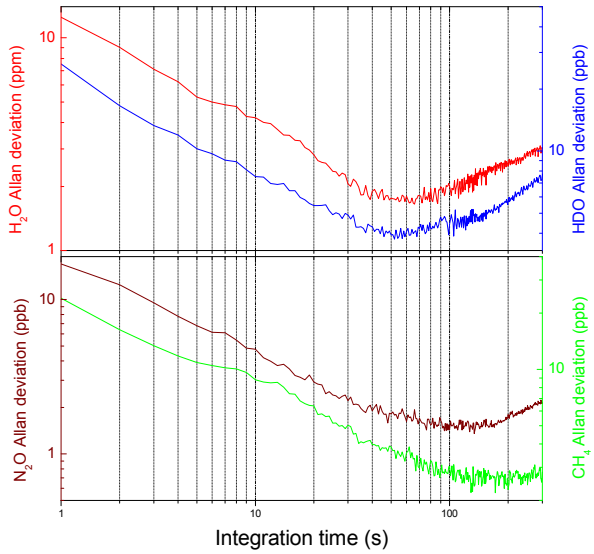

Fig. 6. Allan deviation plots of H_2O (red), HDO (blue), N_2O (wine), and CH_4 (green) concentrations as a function of integration time.

5. Simultaneous detection of atmospheric H_2O, HDO, N_2O and CH_4

The suitability of the developed sensor system for simultaneous monitoring of atmospheric H_2O, HDO, N_2O and CH_4 was demonstrated by conducting a one-week long continuous sampling campaign on the Rice University campus. A sampling line connected to the sensor system was extended to the outside of the Laser Science Group laboratory. Concentration measurements of the four gas species (with a 1-s acquisition time) were performed from February 1 to February 8, 2016. Figure 7 depicts the 1-min averaged time series of the mixing ratios of H_2O, HDO, N_2O, and CH_4 detected simultaneously during this period. The H_2O and HDO vapor concentrations exhibited large variability during the monitoring period. The mixing ratio of HDO varied between 0.53 and 7.0 ppmv, with an average level of 2.2 ± 1.64 (1σ) ppmv, while the H_2O vapor concentration had an average level of 0.74 ± 0.58%. An increase in H_2O and HDO mixing ratios was observed after February 4, 2016, which agreed with increasing ambient temperatures in the Houston area. The large H_2O and HDO concentration levels (above 2% and 7 ppmv, respectively) detected on February 1 were also observed in H_2O vapor concentrations calculated based on meteorological parameters (relative humidity, temperature and atmospheric pressure) retrieved from a Texas Commission on Environmental Quality (TCEQ) station (CAMS 695) located in the proximity of the Rice University campus.

#262458 Received 4 Apr 2016; accepted 29 Apr 2016; published 3 May 2016

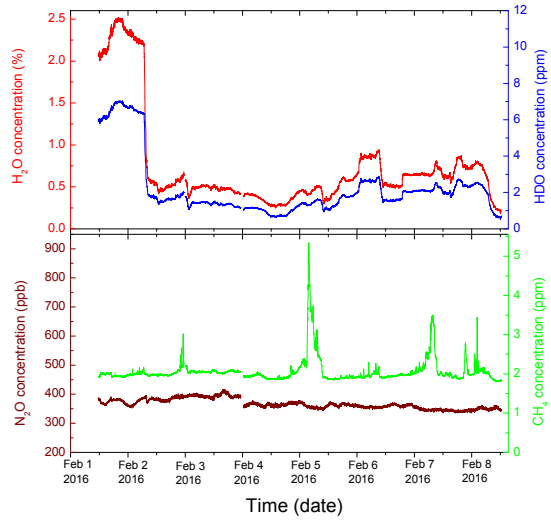

Fig. 7. Time series of H_2O (red), HDO (blue), N_2O (wine), and CH_4 (green) mixing ratios measured on the Rice University campus during February 1-8, 2016.

Although slightly higher H_2O vapor concentrations were detected by our sensor system at some intervals during the sampling period, there is a good relationship (R^2 = 0.98) between the calculated and measured concentration levels for this species shown in Fig. 8. The HDO/H_2O ratio, which provides insight of the processes and dynamics of water vapor in the atmosphere, exhibited small variability during the monitoring period with levels between 2.4 $\times 10^{-4}$ and 3.3 $\times 10^{-4}$ and an average value of $3 \times 10^{-4} \pm 1.9 \times 10^{-5}$. This value indicates that the HDO mixing ratios are ~3000 times smaller than H_2O vapor mixing ratios, which is consistent with the expected abundance of this isotope [23]. In Fig. 7, the levels of N_2O showed minor variability during the interval of monitoring, with mixing ratios ranging between 330 and 410 ppbv and an average mixing ratio of 366 ± 22 ppbv. This value agrees with background levels reported previously for this gas species in the Houston area [2, 7]. The concentration of CH_4 ranged between 1.8 and 5.3 ppmv with an average of 2.06 ± 0.32 ppmv, consistent with typical urban background levels previously observed for this gas species [24]. Large mixing ratios of CH_4, with levels above 5 ppmv, were detected in the early morning of February 5, suggesting a CH_4 emission source close to the Rice Laser Science Group Laboratory during this period.

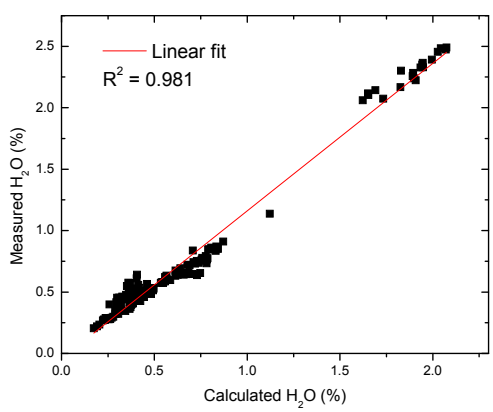

Fig. 8. Comparison of measured 1-hour averaged H_2O vapor mixing ratios with levels calculated based on meteorological data collected at a TCEQ station located in the proximity of the Rice University campus (February 1-8, 2016).

#262458 Received 4 Apr 2016; accepted 29 Apr 2016; published 3 May 2016

Figure 9 shows the diurnal trends of the measured species during the sampling period. The mixing ratios of H_2O and HDO exhibited large hourly variability mainly associated with unusually high levels of these species during the first ~24 h of sampling (February 1, and the early morning of February 2). As mentioned previously, these atypical mixing ratios were also observed in the H_2O vapor levels calculated based on meteorological parameters. The average mixing ratios of H_2O vapor and its heavier isotope followed a similar trend and showed higher levels during nighttime and expected decreased concentrations (associated with increases in ambient temperature) during the daytime. Although a side-by-side pattern can be noticed for the H_2O and HDO hourly variation, the mixing ratios for the latter gas species exhibited a more pronounced pattern. The diurnal profile of N_2O showed a minimum level in the morning hours (~8:00 CDT) with a slight increase in the mixing ratios during daytime. In general, the average concentration level of N_2O exhibited a minor variation (ranging between ~360 and 370 ppbv) during a 24-h period. The diurnal trend of CH_4 mixing ratios showed a marked increase during the early morning hours with a subsequent decrease during the day and a minor secondary peak at ~21:00 CDT. The variability of the CH_4 levels from ~3:00 to 7:00 CDT (time interval of increased concentration for this species) was larger than that observed for periods where CH_4 mixing ratios exhibited similar levels to atmospheric background concentrations (~2 ppmv). The hourly profile for this gas species is consistent with previous reports of CH_4 mixing ratios trends at different urban locations [25, 26]. These results demonstrate the feasibility of the developed sensor system for continuous multi-gas species monitoring as well as its capability of simultaneously capturing distinctive atmospheric behavior and dynamics of H_2O, HDO, N_2O and CH_4.

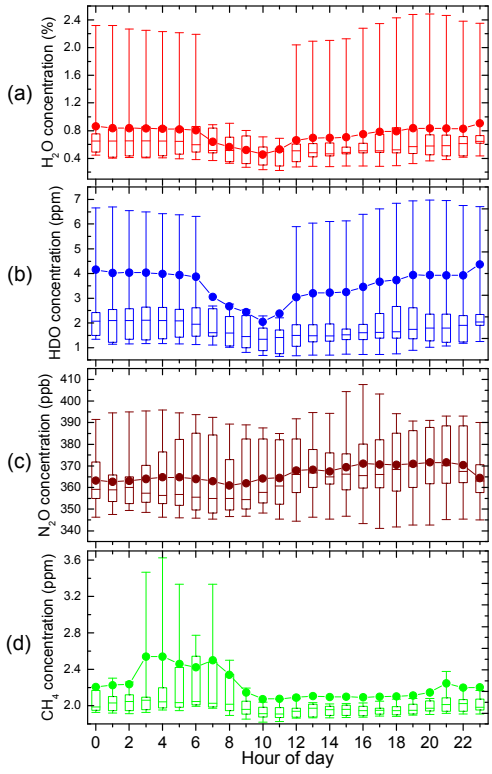

Fig. 9. Diurnal variations of atmospheric (a) H_2O, (b) HDO, (c) N_2O, and (d) CH_4 mixing ratios during the period of monitoring. Bottom whisker, bottom box line, top box line, and top whisker indicate 10th, 25th and 75th, 90th percentile, respectively. Line inside the box and solid circle represent the median and mean values respectively.

#262458 Received 4 Apr 2016; accepted 29 Apr 2016; published 3 May 2016

6. Conclusions

A CW EC-QCL based sensor system for simultaneous detection of atmospheric H_2O, HDO, N_2O, and CH_4 by using a compact MPGC with an effective optical path-length of 57.6 m was developed. The EC-QCL operates at ~7.8 μm in a mode-hop-free spectral range of 1225-1285 cm^{-1}. The spectral tuning of the EC-QCL was calibrated by means of a Ge etalon with a free spectral range (FSR) of 0.0164cm^{-1}. Four interference-free absorption lines were selected within the EC-QCL spectral region at a reduced pressure of 40Torr. A strategy of using 1f-normalized peak-to-peak values of WMS-2f was implemented to process the acquired spectral data. The noise level of the sensor system was evaluated using the Allan-Werle variance method with MDLs of 12.5 ppmv for H_2O, 26.5 ppbv for HDO, 17.0 ppbv for N_2O, and 24.0 ppbv for CH_4 at a 1-s integration time. Furthermore, MDLs of 1.77 ppmv for H_2O, 3.92 ppbv for HDO, 1.43 ppbv for N_2O, and 2.2 ppbv for CH_4 can be achieved with integration times at 50-s, 50-s, 100-s, and 129-s, respectively. The long-term stability of the four-gas sensor was verified by performing a one-week long ambient monitoring campaign on the Rice University campus. The H_2O vapor concentration levels measured showed good agreement with the calculated concentration levels based on meteorological parameters from a nearby TCEQ station. The measurement results indicate that reported TDLAS based sensor system is able to perform the sensitive and precise detection of four non-CO_2 GHGs simultaneously.

Acknowledgments

Yajun Yu acknowledges the financial support from China Scholarship Council (CSC) under the Grant No.201406270063. Nancy Sanchez and Robert Griffin acknowledge support from the Shell Center for Sustainability, the George R. Brown School of Engineering at Rice University and a National Science Foundation (NSF) ERC MIRTHE award. Frank Tittel acknowledges support by a National Science Foundation (NSF) ERC MIRTHE award, a Robert Welch Foundation Grant C-0586, a NSF Phase II SBIR (Grant No. IIP-1230427 as well as DE DE) and DOE ARPA-E awards # DE-0000545 with Aeris Technologies, Inc and # DE-0000547 with Thorlabs, Inc.